

## Accepted Manuscript

Near-infrared (NIR) luminescent hetero-tetranuclear  $Zn_2Ln_2$  ( $Ln = Nd, Yb$  or  $Er$ ) complexes self-assembled from the benzimidazole-based HL and two rigid 4,4'-bipyridine ligands with different spacers

Zhao Zhang, Weixu Feng, Peiyang Su, Han Liu, Yao Zhang, Zheng Wang, Tiezheng Miao, Xingqiang Lü, Daidi Fan, Wai-Kwok Wong, Richard A. Jones

PII: S1386-1425(13)00736-1  
DOI: <http://dx.doi.org/10.1016/j.saa.2013.06.122>  
Reference: SAA 10743

To appear in: *Spectrochimica Acta Part A: Molecular and Biomolecular Spectroscopy*



Please cite this article as: Z. Zhang, W. Feng, P. Su, H. Liu, Y. Zhang, Z. Wang, T. Miao, X. Lü, D. Fan, W-K. Wong, R.A. Jones, Near-infrared (NIR) luminescent hetero-tetranuclear  $Zn_2Ln_2$  ( $Ln = Nd, Yb$  or  $Er$ ) complexes self-assembled from the benzimidazole-based HL and two rigid 4,4'-bipyridine ligands with different spacers, *Spectrochimica Acta Part A: Molecular and Biomolecular Spectroscopy* (2013), doi: <http://dx.doi.org/10.1016/j.saa.2013.06.122>

This is a PDF file of an unedited manuscript that has been accepted for publication. As a service to our customers we are providing this early version of the manuscript. The manuscript will undergo copyediting, typesetting, and review of the resulting proof before it is published in its final form. Please note that during the production process errors may be discovered which could affect the content, and all legal disclaimers that apply to the journal pertain.

**Near-infrared (NIR) luminescent hetero-tetranuclear  
Zn<sub>2</sub>Ln<sub>2</sub> (Ln = Nd, Yb or Er) complexes self-assembled  
from the benzimidazole-based HL and two rigid  
4,4'-bipyridine ligands with different spacers**

Zhao Zhang<sup>a</sup>, Weixu Feng<sup>a\*</sup>, Peiyang Su<sup>a</sup>, Han Liu<sup>a</sup>, Yao Zhang<sup>a</sup>, Zheng Wang<sup>a</sup>,  
Tiezheng Miao<sup>a</sup>, Xingqiang Lü<sup>a,b\*</sup>, Daidi Fan<sup>a</sup>, Wai-Kwok Wong<sup>c</sup>, Richard A. Jones<sup>d</sup>

<sup>a</sup>*Shaanxi Key Laboratory of Degradable Medical Material, Shaanxi Key Laboratory of  
Physico-inorganic Chemistry, Northwest University, Xi'an 710069, Shaanxi, China*

<sup>b</sup>*Fujian Institute of Research on the Structure of Matter, Chinese Academy of Science, Fuzhou  
350002, Fujian, China*

<sup>c</sup>*Department of Chemistry, Hong Kong Baptist University, Waterloo Road, Kowloon Tong,  
Hong Kong, China.*

<sup>d</sup>*Department of Chemistry and Biochemistry, The University of Texas at Austin, 1 University  
Station A5300, Austin, TX 78712-0165, United States*

To whom correspondence should be addressed. Tel./fax: +86-029-88302312

E-mail: [lvxq@nwu.edu.cn](mailto:lvxq@nwu.edu.cn) and [fwxdk@foxmail.com](mailto:fwxdk@foxmail.com)

**Abstract**

Through the self-assembly of the benzimidazole-based ligand **HL** (**HL** = 2-(1H-benzo[d]imidazol-2-yl)-6-methoxyphenol) with  $\text{Zn}(\text{OAc})_2 \cdot 2\text{H}_2\text{O}$ ,  $\text{Ln}(\text{NO}_3)_3 \cdot 6\text{H}_2\text{O}$  ( $\text{Ln}$  = Nd, Yb, Er or Gd) and 4,4'-bipyridine ligand (bpy, 4,4'-bipyridine or bpe, *trans*-bis(4-pyridyl)ethylene), two series of  $\text{Zn}_2\text{Ln}_2$ -arrayed complexes  $[\text{Zn}_2\text{Ln}_2(\text{L})_4(\text{bpy})(\text{NO}_3)_6]$  ( $\text{Ln}$  = Nd, **1**; Yb, **2**; Er, **3** or Gd, **4**) and  $[\text{Zn}_2\text{Ln}_2(\text{L})_4(\text{bpe})(\text{NO}_3)_6]$  ( $\text{Ln}$  = Nd, **5**; Yb, **6**; Er, **7** or Gd, **8**) were obtained, respectively. The result of their photophysical properties shows that the characteristic near-infrared (NIR) luminescence of  $\text{Nd}^{3+}$ ,  $\text{Yb}^{3+}$  or  $\text{Er}^{3+}$  ion has been sensitized from the excited state (both  $^1\text{LC}$  and  $^3\text{LC}$ ) of the mixed **HL** and bipyridyl ligands in both complexes **1-3** and **5-7**. Moreover, the change from bpy to bpe bridging for the fine-tuning of whole molecular conjugations, attributing to the different crossings of the two benzimidazole-based **L** ligands, has the important influence on their NIR luminescent properties.

**Keywords:** Hetero-tetranuclear  $\text{Zn}_2\text{Ln}_2$ -arrayed complexes; Mixed **HL**-bipyridine ligands; Sensitization of NIR luminescence

## 1. Introduction

Much recent research interest has been devoted into near-infrared (NIR) luminescent lanthanide (Ln = Nd, Yb or Er) complexes [1] with the long-lived (ms or  $\mu$ s) lifetime, the large Stokes' shift and the characteristic narrow-line emission [2], which have potential applications in functional devices for NIR organic light-emitting diodes (OLEDs) [3], tele-communication [4] and bio-analysis [5]. However, due to the low absorption coefficients and the low emissive rates of the parity forbidden f-f transitions [6], the introduction of organic chromophores [7] including transition metal complexes [8] as the sensitizers of these Ln<sup>3+</sup> acceptors is necessarily emerging. From the viewpoint of efficient sensitization of Ln<sup>3+</sup>-based NIR luminescence, the choice of suitable chromophores remains an actual challenge, which requires the realization of the energy level's match of the excited state of the chromophores to the Ln<sup>3+</sup> ions' excited state besides the complete avoidance or decrease of the luminescent quenching effect arising from OH-, CH- or NH-containing oscillators around the Ln<sup>3+</sup> ions [9].

It is of special notice that series of 3d Zn<sup>2+</sup> complexes from adeninate [10], hydroxylquinoline [11], imidazoledicarboxylate [12] or tetrazole-based ligands [13], as the chromophores, have been used to effectively sensitize the NIR emission of the Ln<sup>3+</sup> ions, attributed to their strong light-harvesting in the near-UV and visible ranges, the efficient energy transfer from the chromophores to the Ln<sup>3+</sup> ions and the minimization of the non-radiative processes of the Ln<sup>3+</sup> ion. In this regard, our past research results have shown that hetero-binuclear ZnLn [14] or hetero-trinuclear Zn<sub>2</sub>Ln [15] complexes could be obtained from the pure Salen-type Schiff-base ligands, where the Zn<sub>2</sub>Ln-arrayed complexes with two

chromophores endow the enhanced NIR luminescence. On the other hand, the Salen-type Schiff-base ligands with the outer O<sub>2</sub>O<sub>2</sub> moieties from MeO- groups are apt to bind both Zn<sup>2+</sup> and Ln<sup>3+</sup> ions, especially in the presence of anion or multidentate-ligand bridging, series of ZnLn [16], Zn<sub>2</sub>Ln [17], Zn<sub>2</sub>Ln<sub>2</sub> [18] or Zn<sub>4</sub>Ln<sub>2</sub> [19] complexes could be constructed, in which both two or more chromophores and/or two Ln<sup>3+</sup> acceptors with increased energy transfer rates usually lead to the better NIR luminescent properties in contrast to those of hetero-binuclear ZnLn complexes. Moreover, the use of flexible linkers while not the rigid ones of the Salen-type Schiff-base ligands with the outer O<sub>2</sub>O<sub>2</sub> moieties results in the larger NIR quantum yields, due to the more effective intra-molecular energy transfer from the ligand-centered both <sup>3</sup>LC and <sup>1</sup>LC not just <sup>1</sup>LC excited state to the Ln<sup>3+</sup> ions. As a matter of fact, based on the success of hetero-binuclear [Zn(L<sup>n</sup>)<sub>2</sub>Ln(Py)] (Py = pyridine) complexes [20], the benzimidazole-based ligands (HL<sup>n</sup>) are proved also to bind both Zn<sup>2+</sup> ion in the inner *cis*-N<sub>2</sub>O<sub>2</sub> core and Ln<sup>3+</sup> ion in the outer O<sub>2</sub>O<sub>2</sub> moiety, and the Zn<sup>2+</sup> complexes ([Zn(L<sup>n</sup>)<sub>2</sub>(Py)]) with two benzimidazole-based ligands sandwiched through the N,O-chelate mode can sensitize the NIR emission of some Ln<sup>3+</sup> ions. Evidently, if using multidentate bridges (such as 4,4'-bipyridine ligands) in replacement with monodentate Py group at the axial position of Zn<sup>2+</sup> ion, hetero-polynuclear Zn<sub>x</sub>Ln<sub>y</sub> (x > 1 and/or y > 1) complexes based on the benzimidazole-based ligands with two or more chromophores and/or two Ln<sup>3+</sup> acceptors should be obtained, and their improved NIR luminescent emissions are also expected. Herein, two series of complexes [Zn<sub>2</sub>Ln<sub>2</sub>(L)<sub>4</sub>(bpy)(NO<sub>3</sub>)<sub>6</sub>] (Ln = Nd, **1**; Yb, **2**; Er, **3** or Gd, **4**) and [Zn<sub>2</sub>Ln<sub>2</sub>(L)<sub>4</sub>(bpe)(NO<sub>3</sub>)<sub>6</sub>] (Ln = Nd, **5**; Yb, **6**; Er, **7** or Gd, **8**) were obtained from the self-assembly of the benzimidazole-based ligand **HL** (**HL** =

2-(1H-benzo[d]imidazol-2-yl)-6-methoxyphenol),  $\text{Zn}(\text{OAc})_2 \cdot 2\text{H}_2\text{O}$ ,  $\text{Ln}(\text{NO}_3)_3 \cdot 6\text{H}_2\text{O}$  ( $\text{Ln} = \text{Nd}$ , Yb, Er or Gd) and bpy or bpe, and the sensitization mechanism on the NIR luminescence of the  $\text{Ln}^{3+}$  ions were also discussed.

## 2. Experimental Section

### 2.1 Materials and Methods

All chemicals were commercial products of reagent grade and were used without further purification. Elemental analyses were performed on a Perkin-Elmer 240C elemental analyzer. Infrared spectra were recorded on a Nicolet Nagna-IR 550 spectrophotometer in the region  $4000 - 400 \text{ cm}^{-1}$  using KBr pellets.  $^1\text{H}$  NMR spectra were recorded on a JEOL EX270 spectrometer with  $\text{SiMe}_4$  as internal standard in  $\text{CD}_3\text{CN}$  at room temperature. ESI-MS was performed on a Finnigan LCQ<sup>DECA</sup> XP HPLC-MS<sub>n</sub> mass spectrometer with a mass to charge ( $m/z$ ) range of 4000 using a standard electrospray ion source and  $\text{CH}_3\text{CN}$  as solvent. Electronic absorption spectra in the UV/Vis region were recorded with a Cary 300 UV spectrophotometer, and steady-state visible fluorescence, PL excitation spectra on a Photon Technology International (PTI) Alphascan spectrofluorometer and visible decay spectra on a pico-N<sub>2</sub> laser system (PTI Time Master). The quantum yield of the visible luminescence for each sample was determined by the relative comparison procedure, using a reference of a known quantum yield (quinine sulfate in dilute  $\text{H}_2\text{SO}_4$  solution,  $\Phi_{em} = 0.546$ ). NIR emission and excitation in solution were recorded by PTI QM4 spectrofluorometer with a PTI QM4 Near-Infrared InGaAs detector.

## 2.2 Synthesis

### 2.2.1 Synthesis of the benzimidazole-based ligand **HL**

(**HL** = 2-(1H-benzo[d]imidazol-2-yl)-6-methoxyphenol)

The ligand **HL** was prepared according to the improved procedure from the literature [20]. A solution of *o*-vanillin (3.04 g, 20 mmol) in absolute EtOH (10 ml) was added slowly to the solution of *o*-phenylenediamine (2.16 g, 20 mmol) in absolute EtOH (10 ml) under a nitrogen atmosphere, and the resulting mixture was stirred overnight at room temperature. The insoluble orange precipitate was filtered off, and was added to absolute EtOH (20 ml) and the mixture was refluxed for 12 h. After cooling to room temperature, the resulting off-white microcrystalline precipitate was filtered off, washed with absolute EtOH and diethyl ether. Yield: 1.46 g, 61%. Calc. for C<sub>14</sub>H<sub>12</sub>N<sub>2</sub>O<sub>2</sub>: C, 69.99; H, 5.03; N, 11.66%; found: C, 69.91; H, 5.07; N, 11.65%. IR (KBr, cm<sup>-1</sup>): 3337 (b), 1899 (w), 1836 (w), 1768 (w), 1625 (m), 1593 (m), 1532 (m), 1495 (s), 1475 (s), 1463 (s), 1450 (s), 1424 (s), 1391 (s), 1333 (m), 1304 (w), 1281 (m), 1262 (s), 1196 (w), 1181 (w), 1155 (w), 1088 (m), 1060 (s), 1009 (w), 981 (m), 954 (w), 930 (w), 909 (m), 863 (m), 831 (s), 788 (s), 745 (s), 717 (m), 651 (m), 633 (m), 603 (s), 571 (w), 555 (w), 520 (w), 501 (m), 440 (m), 419 (w). <sup>1</sup>H NMR (400 MHz, CD<sub>3</sub>CN):  $\delta$  (ppm) 13.42 (s, 1H, -NH), 13.27 (s, 1H, -OH), 7.67 (d, 1H, -Ph), 7.45 (m, 2H, -Ph), 7.32 (m, 2H, -Ph), 7.10 (d, 1H, -Ph), 6.93 (t, 1H, -Ph), 3.83 (s, 3H, -OMe).

2.2.2 Syntheses of [Zn<sub>2</sub>Ln<sub>2</sub>(L)<sub>4</sub>(bpy)(NO<sub>3</sub>)<sub>6</sub>] (Ln = Nd, **1**; Ln = Yb, **2**; Ln = Er, **3** or Ln = Gd,

**4**)

To a stirred solution of **HL** (95.6 mg, 0.4 mmol) in absolute THF (10 ml), solid

Zn(OAc)<sub>2</sub>·2H<sub>2</sub>O (43.9 mg, 0.2 mmol) and absolute bpy (4,4'-bipyridine, 15.6 mg, 0.1 mmol) were added separately, and the final mixture was heated under reflux for 5 h. A solution of Ln(NO<sub>3</sub>)<sub>3</sub>·6H<sub>2</sub>O (0.2 mmol, Ln = Nd, 0.087 g; Ln = Yb, 0.089 g; Ln = Er, 0.088 g; Ln = Gd, 0.090 g) in absolute MeCN (4 ml) were added, sequentially. Then the mixture was refluxed for another 3 h. The respective yellow clear solution was then cooled to room temperature and filtered. Diethyl ether was allowed to diffuse slowly into the respective solution at room temperature and pale yellow microcrystallines **1-4** were obtained in about three weeks, respectively.

For **1**: Yield: 0.136 g, 68%. Calc. for C<sub>66</sub>H<sub>52</sub>N<sub>16</sub>O<sub>26</sub>Zn<sub>2</sub>Nd<sub>2</sub>: C, 41.62; H, 2.75; N, 11.77%; found: C, 41.53; H, 2.82; N, 11.78%. IR (KBr, cm<sup>-1</sup>): 3421 (w), 3132 (w), 1772 (w), 1658 (m), 1627 (m), 1609 (m), 1538 (m), 1479 (s), 1452 (m), 1403 (m), 1387 (s), 1311 (vs), 1287 (s), 1248 (s), 1203 (m), 1180 (m), 1164 (m), 1121 (w), 1093 (m), 1050 (s), 994 (m), 934 (w), 908 (w), 867 (m), 848 (m), 816 (w), 785 (m), 741 (s), 702 (m), 659 (m), 626 (w), 563 (w), 535 (w), 512 (m), 445 (m), 415 (w). <sup>1</sup>H NMR (400 MHz, CD<sub>3</sub>CN): δ (ppm) 12.27 (s, 4H), 8.85 (d, 4H), 7.71 (s, 4H), 7.04 (m, 8H), 6.82 (m, 4H), 6.65 (m, 4H), 6.12 (s, 4H), 5.60 (s, 4H), 4.73 (m, 4H), -1.96 (s, 12H). ESI-MS (CH<sub>3</sub>CN) m/z: 1905.48 ([M-H]<sup>+</sup>, 100%).

For **2**: Yield: 0.131 g, 67%. Calc. for C<sub>66</sub>H<sub>52</sub>N<sub>16</sub>O<sub>26</sub>Zn<sub>2</sub>Yb<sub>2</sub>: C, 40.40; H, 2.67; N, 11.42%; found: C, 40.28; H, 2.86; N, 11.46%. IR (KBr, cm<sup>-1</sup>): 3468 (w), 1772 (w), 1661 (m), 1628 (s), 1570 (m), 1542 (m), 1530 (m), 1492 (m), 1480 (s), 1453 (m), 1424 (w), 1384 (vs), 1316 (s), 1283 (w), 1257 (w), 1240 (w), 1200 (m), 1180 (m), 1087 (vs), 990 (m), 912 (w), 869 (w), 837 (m), 788 (m), 745 (m), 719 (s), 662 (w), 635 (w), 604 (w), 547 (w), 515 (m), 460 (w), 443 (m), 420 (m). ESI-MS (CH<sub>3</sub>CN) m/z: 1963.08 (100%).

For **3**: Yield: 0.124 g, 64%. Calc. for  $C_{66}H_{52}N_{16}O_{26}Zn_2Er_2$ : C, 40.64; H, 2.69; N, 11.49%; found: C, 40.55; H, 2.77; N, 11.50%. IR (KBr,  $cm^{-1}$ ): 3440 (w), 1772 (w), 1732 (w), 1659 (m), 1637 (m), 1568 (m), 1537 (m), 1496 (m), 1478 (vs), 1463 (m), 1451 (vs), 1424 (m), 1387 (vs), 1335 (w), 1308 (m), 1283 (m), 1260 (s), 1239 (m), 1198 (m), 1185 (m), 1158 (m), 1090 (s), 1059 (s), 993 (m), 933 (w), 909 (w), 864 (w), 834(w), 787 (m), 778 (m), 764 (w), 745 (s), 719 (m), 653 (w), 633 (w), 603 (w), 551 (w), 502 (w), 459 (w), 446 (m), 421 (m). ESI-MS ( $CH_3CN$ ) m/z: 1951.52 (100%).

For **4**: Yield: 0.116 g, 60%. Calc. for  $C_{66}H_{52}N_{16}O_{26}Zn_2Gd_2$ : C, 41.06; H, 2.72; N, 11.61%; found: C, 40.95; H, 2.80; N, 11.62%. IR (KBr,  $cm^{-1}$ ): 3455 (w), 1772 (w), 1660 (s), 1626 (m), 1544 (w), 1535 (w), 1496 (w), 1479 (m), 1450 (m), 1427 (s), 1384 (s), 1309 (s), 1286 (m), 1260 (s), 1242 (w), 1200 (w), 1182 (w), 1085 (vs), 987 (s), 912 (w), 863 (m), 834 (w), 792 (w), 745 (m), 718 (w), 602 (w), 526 (w), 460 (m), 420 (m). ESI-MS ( $CH_3CN$ ) m/z: 1931.50 (100%).

### 2.2.3 Syntheses of $[Zn_2Ln_2(L)_4(bpe)(NO_3)_6]$ ( $Ln = Nd$ , **5**; $Ln = Yb$ , **6**; $Ln = Er$ , **7**; $Ln = Gd$ , **8**)

To a stirred solution of **HL** (95.6 mg, 0.4 mmol) in absolute EtOH (10 ml), solid  $Zn(OAc)_2 \cdot 2H_2O$  (43.9 mg, 0.2 mmol) and absolute bpe (*trans*-1,2-bis(4-pyridyl)ethylene, 18 mg, 0.1 mmol) were added separately, and the final mixture was heated under reflux for 5 h. A solution of  $Ln(NO_3)_3 \cdot 6H_2O$  (0.2 mmol,  $Ln = Nd$ , 0.087 g;  $Ln = Yb$ , 0.089 g;  $Ln = Er$ , 0.088 g;  $Ln = Gd$ , 0.090 g) in absolute MeCN (20 ml) were added sequentially. Then the mixture was refluxed for another 3 h. The respective yellow clear solution was then cooled to room temperature and filtered. Diethyl ether was allowed to diffuse slowly into the respective

solution at room temperature and pale yellow microcrystallines **5-8** were obtained in about three weeks, respectively.

For **5**: Yield: 0.144 g, 75%. Calc. for  $C_{68}H_{54}N_{16}O_{26}Zn_2Nd_2$ : C, 42.31; H, 2.82; N, 11.61%; found: C, 42.20; H, 2.88; N, 11.63%. IR (KBr,  $cm^{-1}$ ): 3122 (m), 2427 (w), 2347 (w), 1649 (m), 1620 (m), 1534 (w), 1479 (s), 1400 (vs), 1387 (vs), 1312 (m), 1240 (m), 1203 (w), 1179 (w), 1163 (w), 1118 (w), 1092 (w), 1053 (m), 1028 (w), 994 (w), 865 (w), 844 (m), 820 (w), 782 (m), 743 (m), 655 (m), 625 (m), 564 (w), 507 (w), 478 (w), 457 (w), 441 (w), 419 (w).  $^1H$  NMR (400 MHz,  $CD_3CN$ ):  $\delta$  (ppm) 13.43 (s, 2H), 13.21 (s, 4H), 8.92 (d, 4H), 7.83 (s, 4H), 7.15 (m, 8H), 6.97 (m, 4H), 6.76 (m, 4H), 6.05 (s, 4H), 5.72 (s, 4H), 4.11 (m, 4H), -2.24 (s, 12H). ESI-MS ( $CH_3CN$ )  $m/z$ : 1931.52 ( $[M-H]^+$ , 100%).

For **6**: Yield: 0.145 g, 73%. Calc. for  $C_{68}H_{54}N_{16}O_{26}Zn_2Yb_2$ : C, 41.08; H, 2.74; N, 11.27%; found: C, 40.96; H, 2.82; N, 11.30%. IR (KBr,  $cm^{-1}$ ): 3436 (w), 3200 (w), 2429 (w), 2342 (w), 1836 (w), 1650 (m), 1623 (m), 1540 (w), 1458 (s), 1396 (vs), 1383 (vs), 1319 (m), 1244 (m), 1198 (w), 1177 (m), 1105 (w), 1056 (m), 1031 (w), 995 (w), 866 (w), 846 (w), 828 (w), 785 (w), 745 (m), 658 (m), 590 (s), 548 (m), 525 (w), 444 (w), 425 (w). ESI-MS ( $CH_3CN$ )  $m/z$ : 1989.12 ( $[M-H]^+$ , 100%).

For **7**: Yield: 0.138 g, 70%. Calc. for  $C_{68}H_{54}N_{16}O_{26}Zn_2Er_2$ : C, 41.32; H, 2.75; N, 11.34%; found: C, 41.21; H, 2.82; N, 11.37%. IR (KBr,  $cm^{-1}$ ): 3413 (w), 3133 (w), 2434 (w), 2370 (w), 2347 (w), 1651 (s), 1623 (s), 1566 (m), 1547 (m), 1480 (s), 1396 (vs), 1381 (vs), 1316 (m), 1291 (w), 1238 (m), 1201 (w), 1176 (w), 1164 (m), 1113 (w), 1093 (w), 1055 (m), 1028 (w), 994 (w), 866 (w), 847 (w), 829 (w), 783(m), 746 (s), 680 (w), 661 (w), 618 (w), 550 (w), 516 (w), 480 (w), 464 (w), 444 (w), 433 (w), 416 (w). ESI-MS ( $CH_3CN$ )  $m/z$ : 1977.56 ( $[M-H]^+$ ,

100%).

For **8**: Yield: 0.133 g, 68%. Calc. for  $C_{68}H_{54}N_{16}O_{26}Zn_2Gd_2$ : C, 41.74; H, 2.78; N, 11.45%; found: C, 41.63; H, 2.85; N, 11.46%. IR (KBr,  $cm^{-1}$ ): 3432 (w), 3139 (w), 2427 (w), 1649 (m), 1625 (s), 1565 (m), 1545 (m), 1480 (m), 1396 (vs), 1379 (vs), 1313 (m), 1281 (w), 1239 (m), 1201 (w), 1179 (w), 1165 (w), 1093 (w), 1057 (s), 1031 (w), 994 (m), 864 (w), 846 (m), 830 (w), 785 (m), 743 (s), 681 (w), 661 (m), 618 (w), 564 (w), 511 (w), 474 (w), 458 (w), 444 (w), 420 (m). ESI-MS ( $CH_3CN$ )  $m/z$ : 1957.54 ( $[M-H]^+$ , 100%).

### 2.3 X-ray crystallography

Single crystals of **1**·3H<sub>2</sub>O and **5**·2EtOH of suitable dimensions were mounted onto thin glass fibers. All the intensity data were collected on a Bruker SMART CCD diffractometer (Mo-K $\alpha$  radiation and  $\lambda = 0.71073 \text{ \AA}$ ) in  $\Phi$  and  $\omega$  scan modes. Structures were solved by Direct methods followed by difference Fourier syntheses, and then refined by full-matrix least-squares techniques against  $F^2$  using SHELXTL [21]. All other non-hydrogen atoms were refined with anisotropic thermal parameters. Absorption corrections were applied using SADABS [22]. All hydrogen atoms were placed in calculated positions and refined isotropically using a riding model. Crystallographic data and refinement parameters for the complexes are presented in Table 1. Relevant atomic distances and bond angles are collected in Table 2. CCDC reference number 934710 (for **1**·3H<sub>2</sub>O) and 929956 (for **5**·2EtOH).

## 3. Results and discussion

### 3.1 Synthesis and characterization

Reaction of *o*-phenylenediamine with *o*-vanillin in 1:1 molar ratio in absolute EtOH at ambient temperature and subsequent refluxing in absolute EtOH, endowed the off-white benzimidazole-based ligand **HL** in 61% yield. Further through the self-assembly of **HL**, Zn(OAc)<sub>2</sub>·2H<sub>2</sub>O, Ln(NO<sub>3</sub>)<sub>3</sub>·6H<sub>2</sub>O (Ln = Nd, Yb, Er or Gd) with bpy or bpe in the molar ratio of 4:2:2:1, two series of eight hetero-tetranuclear Zn<sub>2</sub>Ln<sub>2</sub> complexes [Zn<sub>2</sub>Ln<sub>2</sub>(L)<sub>4</sub>(bpy)(NO<sub>3</sub>)<sub>6</sub>] (Ln = Nd, **1**; Yb, **2**; Er, **3** or Gd, **4**) and [Zn<sub>2</sub>Ln<sub>2</sub>(L)<sub>4</sub>(bpe)(NO<sub>3</sub>)<sub>6</sub>] (Ln = Nd, **5**; Yb, **6**; Er, **7** or Gd, **8**) were obtained, respectively, as shown in Scheme 1.

[Scheme 1 inserted here]

The benzimidazole-based ligand **HL** and two series of Zn<sub>2</sub>Ln<sub>2</sub>-arrayed complexes **1-4** and **5-8** complexes were well characterized by EA, FT-IR, <sup>1</sup>H NMR and ESI-MS. In the FT-IR spectra, the characteristic strong absorptions of the ν(C=N) vibrations [23] of benzimidazole rings at 1661-1658 and 1637-1626 cm<sup>-1</sup> for complexes **1-4** or 1651-1649 and 1625-1623 cm<sup>-1</sup> for complexes **5-8**, respectively, are slightly blue-shifted by the range of 33-36 and 33-44 cm<sup>-1</sup> or 24-26 and 30-33 cm<sup>-1</sup> relative to those (1625 and 1593 cm<sup>-1</sup>) of the free benzimidazole-based ligand **HL** upon the coordination of the metal ions. Moreover, two additional strong absorptions at 1387-1384 and 1316-1308 cm<sup>-1</sup> for complexes **1-4** or 1387-1379 and 1319-1311 cm<sup>-1</sup> for complexes **5-8** were observed, which are typical for the bidentate NO<sub>3</sub><sup>-</sup> groups [23], respectively. As to the room temperature <sup>1</sup>H NMR spectra in CD<sub>3</sub>CN of both complexes **1** and **5**, a large shift (δ from 12.27 to -1.96 for **1**; 13.43 to -2.24 ppm for **5**) of the proton resonances of the two mixed ligands (L<sup>-</sup> and bpy or bpe) to high fields is observed due to the Nd<sup>3+</sup>-induced shift. The down-field signals (δ 12.27 and 8.85 ppm for **1**; δ 13.43, 13.21 and 8.92 ppm for **5**) are assigned to the protons of complexed

4,4'-bipyridine linkers, shifted down-field relatively compared with free bpy ( $\delta$  7.82 and 8.69 ppm) or bpe ( $\delta$  7.48, 7.73 and 8.74 ppm). The signals of the coordinated ligands ( $\delta$  from 7.71 to -1.96 ppm for **1** and  $\delta$  from 7.83 to -2.24 ppm for **5**) are significantly spread relative to those ( $\delta$  from 7.67 to 3.83 ppm) of the free benzimidazole-based ligand **HL**. The ESI-MS spectra of the two series of complexes **1-4** and **5-8** in MeCN display the similar patterns and exhibit the strong mass peak at  $m/z$  1905.48 (**1**), 1963.08 (**2**), 1951.52 (**3**) or 1931.50 (**4**) and 1931.52 (**5**), 1989.52 (**6**), 1977.56 (**7**) or 1957.54 (**8**), assigned to the major species  $\{[\text{Zn}_2\text{Ln}_2(\text{L})_4(\text{bpy})(\text{NO}_3)_6]\text{-H}\}^+$  of complexes **1-4** and  $\{[\text{Zn}_2\text{Ln}_2(\text{L})_4(\text{bpe})(\text{NO}_3)_6]\text{-H}\}^+$  of complexes **5-8**, respectively. These observations further indicate that each of the discrete tetranuclear molecules **1-4** and **5-8** is retained in the respective dilute MeCN solution.

### 3.2 Molecular Structures of Complexes **1**·3H<sub>2</sub>O and **5**·2EtOH

The molecular structures of **1**·3H<sub>2</sub>O as the representative of complexes **1-4** and **5**·2EtOH as the representative of complexes **5-8** were determined by X-ray single-crystal diffraction analysis. Crystallographic data for the two complexes are presented in Table 1, and selected bond lengths and angles are given in Table 2. For complex **1**·3H<sub>2</sub>O, it crystallizes in the monoclinic space group of *C2/c*. As shown in Figure 1, two crystallographically equivalent Zn-Nd moieties lie about the inversion center, and one bpy bridges the two Zn<sup>2+</sup> ions. Each Zn<sup>2+</sup> (Zn1 or Zn1a) ion lies in a common five-coordinate environment and has a distorted square pyramidal geometry, as shown by the same calculated  $\tau$  value [24] of 0.496, where the inner N<sub>2</sub>O<sub>2</sub> core (N2, O2, N3 and O3) from two deprotonated benzimidazole-based L<sup>-</sup> ligands with the same N'O-chelate mode comprises the basal plane, and one terminal N (N5) atom

from the coordinated bpy at the apical position. For each of the two  $\text{Nd}^{3+}$  (Nd1 or Nd1a) ions, it is ten-coordinated, composed of the outer  $\text{O}_2\text{O}_2$  cavity (O1, O2, O3 and O4) from two deprotonated benzimidazole-based  $\text{L}^-$  ligands and six O atoms from three bidentate  $\text{NO}_3^-$  anions. The bond lengths (1.964(19)-2.094(14) Å) of Zn-N (the benzimidazole-based  $\text{L}^-$  ligand) are slightly shorter than that (2.110(13) Å) of Zn-N (N5 of bpy) bond while between those (2.062(10)-2.135(15) Å) of Zn-O (phenoxo, O2 and O3 atoms from two benzimidazole-based  $\text{L}^-$  ligands) bonds. The ten Nd-O bond lengths depend on the nature of the O atoms: they vary from 2.407(11)-2.588(15) Å, and the bond lengths (2.407(11)-2.421(13) Å) from the phenoxo O atoms (O2 and O3) are slightly shorter than those (2.534(14)-2.588(15) or 2.427(16)-2.584(19) Å) from -OMe groups or  $\text{NO}_3^-$  anions. For the tetranuclear  $\text{Zn}_2\text{Nd}_2$ -arrayed complex  $\mathbf{1}\cdot 3\text{H}_2\text{O}$ , the same Zn-Nd distance of each moiety with two benzimidazole-based  $\text{L}^-$  ligands sandwiched is 3.655(3) Å, slightly longer than that (3.636(3) Å) of hetero-binuclear complex  $[\text{ZnNd}(\text{L})_2(\text{Py})(\text{NO}_3)_3]$  from the same benzimidazole-based  $\text{L}^-$  ligand [20], which should be resulted from the larger crossing (118.4(2)° of the dihedral angle between the two benzimidazole rings) of the two benzimidazole-based  $\text{L}^-$  ligands in each moiety. It is worth noting that in the formation of  $\text{Zn}_2\text{Nd}_2$ -arrayed structure of complex  $\mathbf{1}\cdot 3\text{H}_2\text{O}$ , the occupation of bpy at the axial positions of two  $\text{Zn}^{2+}$  ions, is considered to completely avoid the further coordination of OH-, CH- or NH-containing solvents around the two  $\text{Nd}^{3+}$  ions, which is comparable of that of complex  $[\text{Zn}_2\text{Nd}_2(\text{Salen})_2(\text{bpy})(\text{NO}_3)_6]$  from the Salen-type Schiff-base ligand [18c], where the similar Zn...Zn separation of 11.243(4) Å from bridged bpy in complex  $\mathbf{1}\cdot 3\text{H}_2\text{O}$  while the larger dihedral angles (112.9(2)-119.2(2)°) between the two benzimidazole rings and bpy are

observed. The three solvate H<sub>2</sub>O molecules are not bound to the framework, and they exhibit no observed interactions with the host structure. A detailed examination of the crystal packing of complex **1**·3H<sub>2</sub>O reveals that two kinds of complementary intermolecular C23-H23...O12 (3.465(23) Å and 158°) and N1-H1...O13 (2.884(23) Å and 157°) hydrogen bonding, one kind of complementary intermolecular C18-H18...π (3.585(23) Å and 127°) hydrogen bonding and two kind of weak intermolecular π...π interactions (3.479(13)-3.891(15) Å) exist between every two adjacent molecules, thus generating to a 1D polymeric chain (shown in Figure 1S). These chains that run parallel are linked with each other through multiple supramolecular forces involving C5-H5...O6 (3.207(31) Å and 169°), C11-H11...O11 (3.430(42) Å and 149°), N4-H4...O7 (3.089(30) Å and 145°) hydrogen bonds and weak π...π interactions (3.905(15) Å), resulting in a 2D sheet as shown in Figure 2S.

**[Tables 1-2 and Figure 1 inserted here]**

The replacement of 4,4'-bipyridine bridge from bpy to bpe does not lead to a significant change of the hetero-tetranuclear host structure of complex **5**·2EtOH. For complex **5**·2EtOH, it crystallizes in the monoclinic space group of *P2(1)/c*, where one hetero-tetranuclear Zn<sub>2</sub>Nd<sub>2</sub>-arrayed [Zn<sub>2</sub>Ln<sub>2</sub>(L)<sub>4</sub>(bpe)(NO<sub>3</sub>)<sub>6</sub>] host structure and two solvate EtOH molecules comprise the repeating unit. As shown in Figure 2, in the two crystallographically equivalent Zn-Nd moieties, in addition to the axial position of each five-coordinate Zn<sup>2+</sup> (Zn1 or Zn1a) ion occupied by the terminal N (N5 or N5a) atom from the bpe bridge, the similar coordination environments for each Zn<sup>2+</sup> (Zn1 or Zn1a) and each Nd<sup>3+</sup> (Nd1 or Nd1a) ion to those in **1**·3H<sub>2</sub>O are observed. The use of bpe endows the observation of relatively longer Zn...Zn separation of 13.607(8) Å and a distorted trigonal bipyramidal geometry (shown by

the same calculated  $\tau$  value of 0.515) of the two five-coordinate  $Zn^{2+}$  ions, which decreases the dihedral angle ( $75.4(2)^\circ$ ) between the two benzimidazole rings in the both Zn-Nd moieties and dihedral angles ( $46.9(2)$ - $111.1(2)^\circ$ ) between the two benzimidazole rings and bpe in complex **5**·2EtOH. Furthermore, the use of bpe leads to the different crystal packing in complex **5**·2EtOH. As shown in Figure 3S, weak intermolecular  $\pi\cdots\pi$  interactions ( $3.666(11)$  Å) connect every two adjacent molecules to form a polymeric 1D chain. These chains run parallel and are linked with each other through two kinds of intermolecular C33-H33 $\cdots$ O9 ( $3.349(22)$  Å and  $144^\circ$ ) and N7-O9 $\cdots\pi$  ( $4.258(22)$  Å and  $106.9^\circ$ ) hydrogen bonds, leading to the formation of a 2D sheet as shown in Figure 4S. A 3D framework is obtained from the intermolecular N1-H1 $\cdots$ O13 ( $3.038(24)$  Å and  $144^\circ$ ) hydrogen bonding interactions as shown in Figure 5S

[Figure 2 inserted here]

### 3.3 Photophysical Properties of Complexes **1-4** and **5-8**

The photophysical properties of **HL** and two series of complexes **1-4** and **5-8** have been examined in dilute MeCN at room temperature or 77 K, and summarized in Table 3 and Figures 3-7. As shown in Figure 3, the almost identical ligand-centered solution absorption spectra (216-220, 296-298 and 332-334 nm) of complexes **1-4** in the UV-visible region are observed, and the lowest energy absorptions are red-shifted by 16-18 nm upon coordination to  $Zn^{2+}$  and  $Ln^{3+}$  ions as compared to that (316 nm) of the free benzimidazole-based ligand **HL**. It is noticed that the molar absorption coefficients of complexes **1-4** in all the lowest energy bands are about three while not four orders of magnitude larger than that of the **HL** ligand

despite the four coordinated  $L^-$  ligands involved. Moreover, the lowest energy absorptions (332-334 nm) for complexes **1-4** are blue-shifted by 5-8 nm in comparison with those (225-231, 298-301 and 339-340 nm) of the previous Zn-Ln complexes  $[ZnLn(L)_2(Py)(NO_3)_3]$  from the same **HL** ligand [20]. The decreased electronic conjugation of the whole molecule system, assigned to the larger dihedral angle ( $118.4(2)^\circ$ ) between the two benzimidazole rings of two benzimidazole-based  $L^-$  ligands in complex **1**·3H<sub>2</sub>O, is evidently in disagreement with the comparison between the Zn<sub>2</sub>Ln<sub>2</sub> and ZnLn complexes from the almost planar Salen-type Schiff-base ligand with the use of bpy and Py [18c], respectively. For complexes **1-3**, the similar residual visible emission ( $\lambda_{em} = 428$  nm,  $\tau < 1$  ns and  $\Phi_{em} < 10^{-5}$ , almost undetectable) in dilute absolute MeCN solution at room temperature are observed, while photo excitation at the range of 270-360 nm ( $\lambda_{ex} = 340$  nm), as shown in Figure 4, gives rise to the characteristic emissions of Nd<sup>3+</sup> ion ( $^4F_{3/2} \rightarrow ^4I_{J/2}$ ,  $J = 9, 11, 13$ ) for complex **1**, the Yb<sup>3+</sup> ion ( $^2F_{5/2} \rightarrow ^2F_{7/2}$ ) for complex **2** and the Er<sup>3+</sup> ion ( $^4I_{13/2} \rightarrow ^4I_{15/2}$ ) for complex **3** in the NIR region, respectively. For complex **1**, the emissions at 908, 1064 and 1326 nm can be assigned to  $^4F_{3/2} \rightarrow ^4I_{9/2}$ ,  $^4F_{3/2} \rightarrow ^4I_{11/2}$  and  $^4F_{3/2} \rightarrow ^4I_{13/2}$  transitions of the Nd<sup>3+</sup> ion, respectively. As to complexes **2-3**, the strong emission at 978 nm and the weak emission at 1540 nm can be attributed to the  $^2F_{5/2} \rightarrow ^2F_{7/2}$  transition of the Yb<sup>3+</sup> ion and the  $^4I_{13/2} \rightarrow ^4I_{15/2}$  transition of the Er<sup>3+</sup> ion, respectively. Further based on the results of time-resolved luminescent experiments, the three luminescent decay curves can be fitted mono-exponentially with time constants of microseconds (1.24  $\mu$ s for **1**, 12.96  $\mu$ s for **2** and 1.68  $\mu$ s for **3**), manifesting the existence of one luminescent center in the respective solution, and the intrinsic quantum yields  $\Phi_{Ln}$  (0.50% for **1**, 0.65% for **2** and 0.21% for **3**) of the Ln<sup>3+</sup> emissions may be estimated by  $\Phi_{Ln} = \tau_{obs}/\tau_0$ , where  $\tau_{obs}$  is the observed

emission lifetime and  $\tau_0$  is the “neutral lifetime” *viz.* 0.25 ms, 2.0 and 8.0 ms for the Nd<sup>3+</sup>, Yb<sup>3+</sup> and Er<sup>3+</sup> ions [25], respectively. For complex **4**, it does not exhibit NIR luminescent emission under the same condition, while the typical ligand-centered fluorescence ( $\lambda_{em} = 428$  nm  $\tau = 1.54$  ns and  $\phi_{em} = 0.33 \times 10^{-3}$ ) in the visible region is observed, as shown in Figure 5. It is worth noting that the similar excitation spectrum ( $\lambda_{ex} = 340$  nm) monitored at the respective strongest NIR emission peak (1064 nm for **1**, 978 nm for **2** or 1540 nm for **3**) to that at the visible emission peak (428 nm) of complex **4**, clearly shows that both the NIR emissions are originated from the same  $\pi$ - $\pi^*$  transitions of the ligands for complexes **1-3**. This also suggests that the energy transfer from the antenna to the Ln<sup>3+</sup> ions takes place efficiently [26].

[Table 3 and Figures 3-4 inserted here]

It is of special interest to explore the mechanism of energy transfer process on the NIR luminescent complexes **1-3**. As a reference compound, complex **4** allows the further study of the antenna luminescence in the absence of energy transfer, because the Gd<sup>3+</sup> ion has no energy levels below 32000 cm<sup>-1</sup>, and therefore cannot accept any energy from the antennae excited state [27]. In dilute MeCN solution at 77 K, complex **4** displays the strengthened antennae fluorescence, showing the higher luminescent intensity ( $\lambda_{em} = 413$  nm and 464 nm) and the distinctively longer luminescence lifetimes (2.35 ns and 3.84 ms). This result shows that the sensitization of the NIR luminescence for complexes **1-3** should arise from both the <sup>1</sup>LC (24213 cm<sup>-1</sup>) and the <sup>3</sup>LC (21552 cm<sup>-1</sup>) excited state of the mixed **HL**-bpy ligands at low temperature while not the simple intra-ligand <sup>1</sup> $\pi$ - $\pi^*$  to <sup>3</sup> $\pi$ - $\pi^*$  transition of each ligand [28]. If the antennae luminescence lifetime of complex **4** is to represent the excited-state lifetime in the absence of the energy transfer, the energy transfer rate ( $k_{ET}$ ) in the complexes **1-3** can thus

be calculated from  $k_{ET} = 1/\tau_q - 1/\tau_u$  [29], where  $\tau_q$  is the residual fluorescence lifetime, and  $\tau_u$  is the fluorescence lifetime in the reference complex **4**, so the energy transfer rates for the  $\text{Nd}^{3+}$ ,  $\text{Yb}^{3+}$  and  $\text{Er}^{3+}$  ions in complexes **1-3** may all be estimated to be above  $5 \times 10^8 \text{ s}^{-1}$ , which could well imply the reason to the effective energy transfer for complexes **1-3**. Furthermore, from the viewpoint of the energy level match, in spite of the effective energy transfer taking place in complex **3**, the larger energy gap between the energy-donating  $^3\text{LC}$  ( $21552 \text{ cm}^{-1}$ ) and the emitting level ( $^4\text{I}_{13/2}$ ,  $6494 \text{ cm}^{-1}$ ) of  $\text{Er}^{3+}$  ion than those ( $^4\text{F}_{3/2}$ ,  $11013 \text{ cm}^{-1}$  of the  $\text{Nd}^{3+}$  ion and  $^2\text{F}_{5/2}$ ,  $10225 \text{ cm}^{-1}$  of  $\text{Yb}^{3+}$  ion) of complexes **1-2** results in the great non-radiative energy loss during the energy transfer, which should be the reason to the weaker NIR luminescence for complex **3** ( $\Phi_{\text{Ln}} = 0.21\%$ ). As the reason to the higher intrinsic quantum yield  $\Phi_{\text{Ln}}$  (0.65%) of the  $\text{Yb}^{3+}$  emission for **2** than that (0.50%) of the  $\text{Nd}^{3+}$  emission for **1**, the excited state of the  $\text{Nd}^{3+}$  ions in **1** is more sensitive to quenching by the nearby and distant C-H oscillators of **HL** and bpy [30] besides the less opportunities of non-radiative migration from the single emitting transition ( $^2\text{F}_{5/2} \rightarrow ^2\text{F}_{7/2}$ ) of the  $\text{Yb}^{3+}$  ion in **3**, although the energy gap ( $^4\text{F}_{3/2}$ ,  $11013 \text{ cm}^{-1}$ ) of the  $\text{Nd}^{3+}$  ion in **2** is smaller than that ( $^2\text{F}_{5/2}$ ,  $10225 \text{ cm}^{-1}$ ) of  $\text{Yb}^{3+}$  ion in **3**.

[Figure 5 inserted here]

Changing the bridge from bpy to more rigid bpe does not extend the conjugation of the whole molecule systems of complexes **5-8** as expected. On the contrary, the decrease of dihedral angle (from  $118.4(2)^\circ$  to  $74.2^\circ$ ) between the two benzimidazole rings of the two benzimidazole-based **L** ligands for complex **5·2EtOH** arisen from the coordination geometry change of the five-coordinate  $\text{Zn}^{2+}$  ions, should be responsible for the lower conjugation, which can be shown the slight blue-shift of the lowest energy absorptions (327-330 nm,

shown in Figure 6) for complexes **5-8** in comparison with those (332-334 nm) of complexes **1-4**. Similarly, for complexes **5-7**, photo excitation at the range of 250-400 nm ( $\lambda_{ex} = 351$  nm), as shown in Figure 7, leads to the characteristic emissions of Nd<sup>3+</sup> ion ( ${}^4F_{3/2} \rightarrow {}^4I_{J/2}$ ,  $J = 9, 11, 13$ ) for complex **5**, the Yb<sup>3+</sup> ion ( ${}^2F_{5/2} \rightarrow {}^2F_{7/2}$ ) for complex **6** and the Er<sup>3+</sup> ion ( ${}^4I_{13/2} \rightarrow {}^4I_{15/2}$ ) for complex **7** in the NIR region, respectively. Similarly, through the further investigation on the emission of the reference complex **8**, especially at 77 K, the existence of both nanosecond (2.26 ns,  $\lambda_{em} = 405$  nm) and microsecond (3.42 ms,  $\lambda_{em} = 455$  nm) luminescence lifetimes also shows the sensitization procedure of the NIR luminescence for the bpe-bridged complexes **5-7** should resulted from both the  ${}^1LC$  (24691 cm<sup>-1</sup>) and the  ${}^3LC$  (21978 cm<sup>-1</sup>) excited state of the mixed **HL**-bpe ligands at low temperature. Moreover, the smaller energy level gap between the energy-donating  ${}^3LC$  (21978 cm<sup>-1</sup>) and the emitting level ( ${}^4F_{3/2}$ , 11013 cm<sup>-1</sup> of the Nd<sup>3+</sup> ion or  ${}^2F_{5/2}$ , 10214 cm<sup>-1</sup> of Yb<sup>3+</sup> ion) in complex **5** or **6** than that ( ${}^4I_{13/2}$ , 6451 cm<sup>-1</sup>) of Er<sup>3+</sup> ion of complex **7** ( $\Phi_{em} = 0.13\%$ ) leads to the stronger NIR luminescence for complexes **5-6** ( $\Phi_{Ln} = 0.61\%$  for **5** and  $\Phi_{Ln} = 0.43\%$  for **6**). It is worth noting that the NIR intrinsic quantum yields  $\Phi_{Ln}$  (Ln = Nd, Yb or Er) of both complexes **1-3** and **5-7** are slightly lower than those of hetero-binuclear [ZnLn(L)<sub>2</sub>(Py)(NO<sub>3</sub>)<sub>3</sub>] complexes [20], respectively, which should be due to the distinctive decrease of the conjugation of the whole Zn<sub>2</sub>Ln<sub>2</sub>-arrayed molecule system in the presence of bpy or bpe, although two chromophores and two acceptors are involved besides the similarly complete avoidance of the luminescent quenching effect arising from OH-, CH- or NH-containing oscillators around the two Ln<sup>3+</sup> ions. This is evidently disagreeable to the comparison between the Zn<sub>2</sub>Ln<sub>2</sub> and ZnLn complexes from the almost planar Salen-type Schiff-base ligand with the use of bpy or bpe and Py [18c], respectively. As

to the higher NIR intrinsic quantum yields  $\Phi_{Ln}$  for **1-3** from bpy than those of **5-8** from bpe, respectively, attributing to the more suitable energy match between the energy-donating  $^3LC$  and the emitting level of the respective  $Ln^{3+}$  ion, it can be shown from the larger crossing of the two benzimidazole-based ligands in complexes **1-3**.

[Figures 6-7 inserted here]

#### 4. Conclusions

In conclusion, two series of  $Zn_2Ln_2$ -arrayed complexes  $[Zn_2Ln_2(L)_4(bpy)(NO_3)_6]$  ( $Ln = Nd, \mathbf{1}; Yb, \mathbf{2}; Er, \mathbf{3}$  or  $Gd, \mathbf{4}$ ) and  $[Zn_2Ln_2(L)_4(bpe)(NO_3)_6]$  ( $Ln = Nd, \mathbf{5}; Yb, \mathbf{6}; Er, \mathbf{7}$  or  $Gd, \mathbf{8}$ ) were obtained from the self-assembly of the benzimidazole-based **HL** with  $Zn(OAc)_2 \cdot 2H_2O$ ,  $Ln(NO_3)_3 \cdot 6H_2O$  and 4,4'-bipyridine ligand (bpy or bpe), respectively, where two chromophores and two  $Ln^{3+}$  acceptors are involved besides the similarly complete avoidance of the luminescent quenching effect arising from OH-, CH- or NH-containing oscillators around the two  $Ln^{3+}$  ions. The result of their photophysical properties shows that the characteristic near-infrared (NIR) luminescence of  $Nd^{3+}$ ,  $Yb^{3+}$  or  $Er^{3+}$  ion has been sensitized from the excited state (both  $^1LC$  and  $^3LC$ ) of the mixed **HL** and bipyridyl ligands in both complexes **1-3** and **5-7**, and the change from bpy to bpe bridging for the difference of whole molecular conjugations, endows the fine-tuning of their NIR luminescent properties. While in facilitating the NIR sensitization, the specific design of hetero-polynuclear complexes from the benzimidazole-based ligands and other second linkers is now under way.

#### Acknowledgements

This work is funded by the National Natural Science Foundation (912222201, 21173165,

20871098), the Program for New Century Excellent Talents in University from the Ministry of Education of China (NCET-10-0936), the State Key Laboratory of Structure Chemistry (20100014), the Provincial Natural Foundation (2011JQ2011) of Shaanxi, the Education Committee Foundation of Shaanxi Province (11JK0588), Graduate Innovation and Creativity Fund (YZZ12038) of Northwest University, Hong Kong Research Grants Council (HKBU 202407 and FRG/06-07/II-16) in P. R. of China.

#### Appendix A. Supplementary data

The crystal packing diagrams for complexes **1**·3H<sub>2</sub>O and **5**·2EtOH are shown in Figures 1-5S of Supporting information. The crystallographic data for complexes **1**·3H<sub>2</sub>O and **5**·2EtOH have been deposited at the Cambridge Crystallographic Data Center, CCDC-934710 (for **1**·3H<sub>2</sub>O) and CCDC-929956 (for **5**·2EtOH). The data can be obtained free of charge via <http://www.ccdc.cam.ac.uk/conts/retrieving.html> or from the Cambridge CB21EZ, UK.

#### References

- [1] T. Nishioka, K. Fukui, K. Matsumoto, in: K. A. Gschneidner, Jr, J.-C. G. Bünzli, V. K. Pecharsky (Eds.), *Handbook on the Physics and Chemistry of Rare Earths*, 37, Elsevier Science B. V., Amsterdam, 2007.
- [2] S. Comby, J.-C. G. Bünzli, in: K. A. Gschneidner Jr, J.-C. G. Bünzli, V. K. Pecharsky (Eds.), *Handbook on the Physics and Chemistry of Rare Earths*, 37, Elsevier Science B. V., Amsterdam, 2007.
- [3] (a) J. Kido, Y. Okamoto, *Chem. Rev.* 102 (2002) 2357-2368;

- (b) M. A. Katkova, M. N. Bochkarev, Dalton Trans. 39 (2010) 6599-6612.
- [4] J.-C. G. Bünzli, S. V. Eliseeva, J. Rare Earths 28 (2010) 824-842.
- [5] J.-C. G. Bünzli, Chem. Rev. 110 (2010) 2729-2755.
- [6] C. Görrler-Walrand, K. Binnemans, in: K. A. Gschneidner Jr, L. Eyring (Eds.), *Handbook on the Physics and Chemistry of Rare Earths*, 23, Elsevier Science B. V., Amsterdam, 1996.
- [7] J.-C. G. Bünzli, C. Piguet, Chem. Soc. Rev. 34 (2005) 1048-1077.
- [8] (a) M. D. Ward, Coord. Chem. Rev. 251 (2007) 1663-1677;  
(b) F. F. Chen, Z. Q. Chen, Z. Q. Bian, C. H. Huang, Coord. Chem. Rev. 254 (2010) 991-1010;  
(c) M. D. Ward, Coord. Chem. Rev. 254 (2010) 2634-2642;  
(d) Y. Liu, M. Pan, Q. Y. Yang, L. Fu, K. Li, S. C. Wei, C. Y. Su, Chem. Mater. 24 (2012) 1954-1960.
- [9] L. Winkless, R. H. C. Tan, Y. Zheng, M. Motevalli, P. B. Wyatt, W. P. Gillin, Appl. Phys. Lett. 89 (2006) 111115-1-3.
- [10] J. An, C. M. Shade, D. A. Chengelis-Czegán, S. Petoud, N. L. Rosi, J. Am. Chem. Soc. 133 (2011) 1220-1223.
- [11] H. B. Xu, H. M. Wen, Z. H. Chen, J. Li, L. X. Shi, Z. N. Chen, Dalton Trans. 39 (2010) 1948-1953.
- [12] (a) Z. G. Gu, H. C. Fang, P. Y. Yin, L. Tong, Y. Ying, S. J. Hu, W. S. Li, Y. P. Cai, Cryst. Growth & Des. 11 (2011) 2220-2227;  
(b) S. M. Li, X. J. Zheng, D. Q. Yuan, A. Ablet, L. P. Jin, Inorg. Chem. 51 (2012)

1201-1203.

- [13] L. Liang, G. Peng, L. Ma, L. Sun, H. Deng, H. Li, W. S. Li, *Cryst. Growth & Des.* 12 (2012) 1151-1158.
- [14] W. X. Feng, Y. N. Hui, T. Wei, X. Q. Lü, J. R. Song, Z. N. Chen, S. S. Zhao, W.-K. Wong, R. A. Jones, *Inorg. Chem. Commun.* 14 (2011) 75-78.
- [15] (a) W. Y. Bi, T. Wei, X. Q. Lü, Y. N. Hui, J. R. Song, S. S. Zhao, W.-K. Wong, R. A. Jones, *New J. Chem.* 33 (2009) 2326-2334;  
(b) Y. N. Hui, W. X. Feng, T. Wei, X. Q. Lü, J. R. Song, S. S. Zhao, W.-K. Wong, R. A. Jones, *Inorg. Chem. Commun.* 14 (2011) 200-204.
- [16] (a) W. K. Lo, W.-K. Wong, W.-Y. Wong, J. P. Guo, K.-T. Yeung, Y.-K. Cheng, X. P. Yang, R. A. Jones, *Inorg. Chem.* 45 (2006) 9315-9325;  
(b) W. Y. Bi, X. Q. Lü, W. L. Chai, J. R. Song, W.-K. Wong, X. P. Yang, R. A. Jones, Z. *Anorg. Allg. Chem.* 634 (2008) 1795-1800;  
(c) W. Y. Bi, X. Q. Lü, W. L. Chai, J. R. Song, W.-Y. Wong, W.-K. Wong, R. A. Jones, J. *Mol. Struct.* 891 (2008) 450-455.
- [17] (a) S. S. Zhao, X. Q. Lü, A. X. Hou, W.-Y. Wong, W.-K. Wong, X. P. Yang, R. A. Jones, *Dalton Trans.* 43 (2009) 9595-9602;  
(b) Y. Zhang, W. X. Feng, H. Liu, Z. Zhang, X. Q. Lü, J. R. Song, D. D. Fan, W.-K. Wong, R. A. Jones, *Inorg. Chem. Commun.* 24 (2012) 148-152.
- [18] (a) X. P. Yang, R. A. Jones, V. Lynch, M. M. Oye, A. L. Holmes, *Dalton Trans.* 5 (2005) 849-851;  
(b) W. K. Wong, X. P. Yang, R. A. Jones, J. H. Rivers, V. Lynch, W.-K. Lo, D. Xiao, M.

- M. Oye, A. L. Holmes, *Inorg. Chem.* 45 (2006) 4340-4345;
- (c) X. Q. Lü, W. Y. Bi, W. L. Chai, J. R. Song, J. X. Meng, W.-Y. Wong, W.-K. Wong, R. A. Jones, *New J. Chem.* 32 (2008) 127-131;
- (d) X. Q. Lü, W. X. Feng, Y. N. Hui, T. Wei, J. R. Song, S. S. Zhao, W.-Y. Wong, W.-K. Wong, R. A. Jones, *Eur. J. Inorg. Chem.* (2010) 2714-2722.
- [19] (a) X. P. Yang, R. A. Jones, W.-K. Wong, V. Lynch, M. M. Oye, A. L. Holmes, *Chem. Commun.* 17 (2006) 1836-1838;
- (b) X. Q. Lü, W. Y. Bi, W. L. Chai, J. R. Song, J. X. Meng, W.-Y. Wong, W.-K. Wong, X. P. Yang, R. A. Jones, *Polyhedron*, 28 (2009) 27-32.
- [20] (a) G. X. Shi, W. X. Feng, D. Zou, X. Q. Lü, Z. Zhang, Y. Zhang, D. D. Fan, S. S. Zhao, W.-K. Wong, R. A. Jones, *Inorg. Chem. Commun.* 22 (2012) 126-130;
- (b) D. Zou, W. X. Feng, G. X. Shi, X. Q. Lü, Z. Zhang, Y. Zhang, H. Liu, D. D. Fan, W.-K. Wong, R. A. Jones, *Spectrochim. Acta A* 98 (2012) 359-366.
- [21] G. M. Sheldrick, *SHELXS-97: Program for Crystal Structure Refinement*, Göttingen, Germany, 1997.
- [22] G. M. Sheldrick, *SADABS*, University of Göttingen, 1996.
- [23] K. Nakamoto, *Infrared and Raman Spectra and Inorganic and Coordination Compounds*, 4<sup>th</sup> Ed., Wiley, New York, 1986.
- [24] M.-A. Munoz-Hernandez, T. S. Keizer, P. Wei, S. Parkin, D. A. Atwood, *Inorg. Chem.* 40 (2001) 6782-6787.
- [25] M. J. Weber, *Phys. Rev.* 171 (1968) 283-291.
- [26] (a) M. Albrecht, O. Osetska, J. Klankermayer, R. Fröhlich, F. Gumy, J.-C. G. Bünzli,

Chem. Commun. 18 (2007) 1834-1836;

(b) M. Pan, M. H. Lan, X. T. Wang, C. Yan, Y. Liu, C. Y. Su, *Inorg. Chim. Acta* 363 (2010) 3757-3764.

[27] W. T. Carnall, P. R. Fields, K. Rajnak, *J. Chem. Phys.* 49 (1968) 4443-4446.

[28] A. Y. Freidzon, A. V. Scherbinin, A. A. Bagaturyants, M. V. Alfimov, *J. Phys. Chem. A* 115 (2011) 4565-4573.

[29] D. L. Dexter, *J. Chem. Phys.* 21 (1953) 836-850.

[30] A. Beeby, I. M. Clarkson, R. S. Dockins, S. Faulkner, D. Parker, L. Royle, A. S. de Souda, J. A. G. Williams, M. Woods, *J. Chem. Soc., Perkin Trans. 2* (1999) 493-504.

ACCEPTED MANUSCRIPT

**Table 1** Crystal data and refinement for **1**·3H<sub>2</sub>O and **5**·2EtOH

Compound	<b>1</b> ·3H <sub>2</sub> O	<b>5</b> ·2EtOH
Empirical formula	C <sub>66</sub> H <sub>64</sub> N <sub>16</sub> Nd <sub>2</sub> O <sub>32</sub> Zn <sub>2</sub>	C <sub>72</sub> H <sub>66</sub> N <sub>16</sub> O <sub>28</sub> Zn <sub>2</sub> Nd <sub>2</sub>
Formula weight	2012.55	2022.63
Crystal system	Monoclinic	Monoclinic
Space group	<i>C2/c</i>	<i>P2(1)/c</i>
<i>a</i> /Å	21.959(9)	21.506(13)
<i>b</i> /Å	19.270(8)	11.461(7)
<i>c</i> /Å	26.659(11)	20.955(14)
<i>α</i> /°	90	90
<i>β</i> /°	90.092(7)	95.469(16)
<i>γ</i> /°	90	90
<i>V</i> /Å <sup>3</sup>	11281(8)	5141(6)
<i>Z</i>	4	2
<i>ρ</i> /g·cm <sup>-3</sup>	1.185	1.307
Crystal size/mm	0.42 × 0.32 × 0.23	0.43 × 0.35 × 0.29
<i>μ</i> (Mo- <i>Kα</i> )/mm <sup>-1</sup>	1.393	1.525
Data/restraints/parameters	12723/6/498	9954/31/530
Quality-of-fit indicator	1.061	0.910
No. Unique reflections	12723	9954
No. Observed reflections	31824	26582
Final <i>R</i> indices [ <i>I</i> >2σ( <i>I</i> )]	<i>R</i> <sub>1</sub> = 0.1486 <i>wR</i> <sub>2</sub> = 0.3621	<i>R</i> <sub>1</sub> = 0.1132 <i>wR</i> <sub>2</sub> = 0.2512
<i>R</i> indices (all data)	<i>R</i> <sub>1</sub> = 0.3403 <i>wR</i> <sub>2</sub> = 0.4624	<i>R</i> <sub>1</sub> = 0.3068 <i>wR</i> <sub>2</sub> = 0.3530

**Table 2** Interatomic distances (Å) and bond angles (°) with esds for complexes **1**·3H<sub>2</sub>O and**5**·2EtOH

1·3H <sub>2</sub> O			5·2EtOH				
Zn(1)-N(2)	1.964(19)	N(2)-Zn(1)-N(3)	109.2(6)	Zn(1)-N(2)	2.040(20)	N(2)-Zn(1)-N(3)	108.3(7)
Zn(1)-N(3)	2.094(14)	N(2)-Zn(1)-N(5)	91.5(6)	Zn(1)-N(3)	1.985(16)	N(2)-Zn(1)-N(5)	93.4(6)
Zn(1)-N(5)	2.110(13)	N(2)-Zn(1)-O(2)	87.4(5)	Zn(1)-N(5)	2.125(9)	N(2)-Zn(1)-O(2)	88.5(5)
Zn(1)-O(2)	2.062(10)	N(2)-Zn(1)-O(3)	162.5(5)	Zn(1)-O(2)	2.073(11)	N(2)-Zn(1)-O(3)	163.1(6)
Zn(1)-O(3)	2.135(15)			Zn(1)-O(3)	2.130(12)		
		O(1)-Nd(1)-O(4)	153.7(5)			O(1)-Nd(1)-O(4)	174.8(4)
Nd(1)-O(1)	2.534(14)	O(2)-Nd(1)-O(3)	65.0(4)	Nd(1)-O(1)	2.552(12)	O(2)-Nd(1)-O(3)	65.7(4)
Nd(1)-O(2)	2.421(13)	O(5)-Nd(1)-O(7)	49.2(5)	Nd(1)-O(2)	2.393(12)	O(5)-Nd(1)-O(7)	51.0(6)
Nd(1)-O(3)	2.407(11)	O(8)-Nd(1)-O(10)	52.0(6)	Nd(1)-O(3)	2.310(12)	O(8)-Nd(1)-O(10)	51.5(5)
Nd(1)-O(4)	2.588(15)	O(11)-Nd(1)-O(13)	49.9(5)	Nd(1)-O(4)	2.821(12)	O(11)-Nd(1)-O(13)	51.0(5)
Nd(1)-O(5)	2.514(13)			Nd(1)-O(5)	2.501(16)		
Nd(1)-O(7)	2.584(19)			Nd(1)-O(7)	2.450(20)		
Nd(1)-O(8)	2.527(17)			Nd(1)-O(8)	2.520(14)		
Nd(1)-O(10)	2.427(16)			Nd(1)-O(10)	2.540(14)		
Nd(1)-O(11)	2.559(16)			Nd(1)-O(11)	2.575(16)		
Nd(1)-O(13)	2.555(13)			Nd(1)-O(13)	2.520(18)		

**Table 3** The photophysical properties of **HL** and complexes **1-8** at  $2 \times 10^{-5}$  M in absolute MeCN solution at room temperature or 77 K

Compound	Absorption	Excitation	Emission
	$\lambda_{ab}/nm$ [ $\log(\epsilon/dm^3mol^{-1}cm^{-1})$ ]	$\lambda_{ex}/nm$	$\lambda_{em}/nm$ ( $\tau$ , $\Phi \times 10^3$ )
<b>HL</b>	219(0.45), 301(0.26), 316(0.17)	364	434(s)
<b>1</b>	220(1.58), 296(0.82), 334(0.61)	340	427(w), 908(1.23, $\mu s$ ), 1064(1.24 $\mu s$ ), 1326(1.26 $\mu s$ )
<b>2</b>	220(1.67), 298(0.83), 332(0.61)	340	428(w), 978(12.96 $\mu s$ )
<b>3</b>	216(1.43), 298(0.74), 332(0.61)	338	430(w), 1540(1.68 $\mu s$ )
<b>4</b>	220(1.58), 296(0.79), 332(0.58)	343	428(m, 1.54 ns, 0.33) 413(s, 2.35 ns, 77K), 464(s, 3.84 ms, 77K)
<b>5</b>	217(1.01), 300(0.59), 330(0.37)	351	422(w), 908(1.05, $\mu s$ ), 1063(1.08 $\mu s$ ), 1325(1.11 $\mu s$ )
<b>6</b>	217(1.09), 298(0.57), 328(0.36)	351	423(w), 979(12.22 $\mu s$ )
<b>7</b>	216(1.18), 299(0.56), 327(0.38)	351	422(w), 1550(1.44 $\mu s$ )
<b>8</b>	214(0.94), 300(0.58), 330(0.36)	353	420(m, 1.12 ns, 0.16) 405(s, 2.26 ns, 77K), 455(s, 3.42 ms, 77K)

## Captions to Scheme and Figures

**Scheme 1** Controlled self-assembly of two series of hetero-tetranuclear  $Zn_2Ln_2$ -arrayed complexes **1-4** and **5-8**

**Figure 1** Perspective drawing of complex **1**·3H<sub>2</sub>O with 15% probability ellipsoids, H atoms and solvates are omitted for clarity

**Figure 2** Perspective drawing of complex **5**·2EtOH with 15% probability ellipsoids, H atoms and solvates are omitted for clarity

**Figure 3** UV-Visible absorption spectra of **HL** and complexes **1-4** in MeCN solution at  $2 \times 10^{-5}$  M at room temperature

**Figure 4** NIR emission and excitation spectra of complexes **1-3** ( $\lambda_{ex} = 340$  nm for **1**,  $\lambda_{ex} = 340$  nm for **2** and  $\lambda_{ex} = 338$  nm for **3**) in MeCN solution at  $2 \times 10^{-5}$  M at room temperature

**Figure 5** Visible emission and excitation spectra of **HL** ( $\lambda_{ex} = 364$  nm), complexes **4** ( $\lambda_{ex} = 343$  nm) and **8** ( $\lambda_{ex} = 353$  nm) in MeCN solution at  $2 \times 10^{-5}$  M at room temperature

**Figure 6** UV-Visible absorption spectra of **HL** and complexes **5-8** in MeCN solution at  $2 \times 10^{-5}$  M at room temperature

**Figure 7** NIR emission and excitation spectra of complexes **5-7** ( $\lambda_{\text{ex}} = 351$  nm) in MeCN

solution at  $2 \times 10^{-5}$  M at room temperature

ACCEPTED MANUSCRIPT

Scheme 1

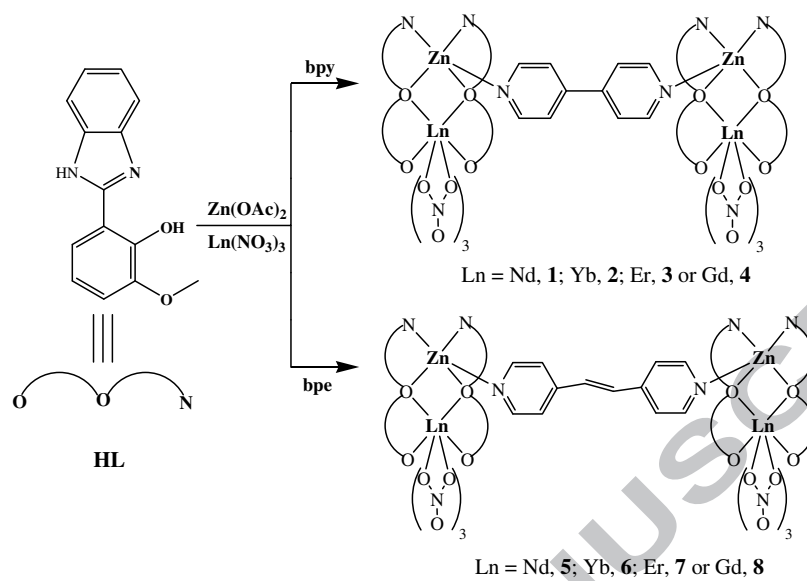


Figure 1

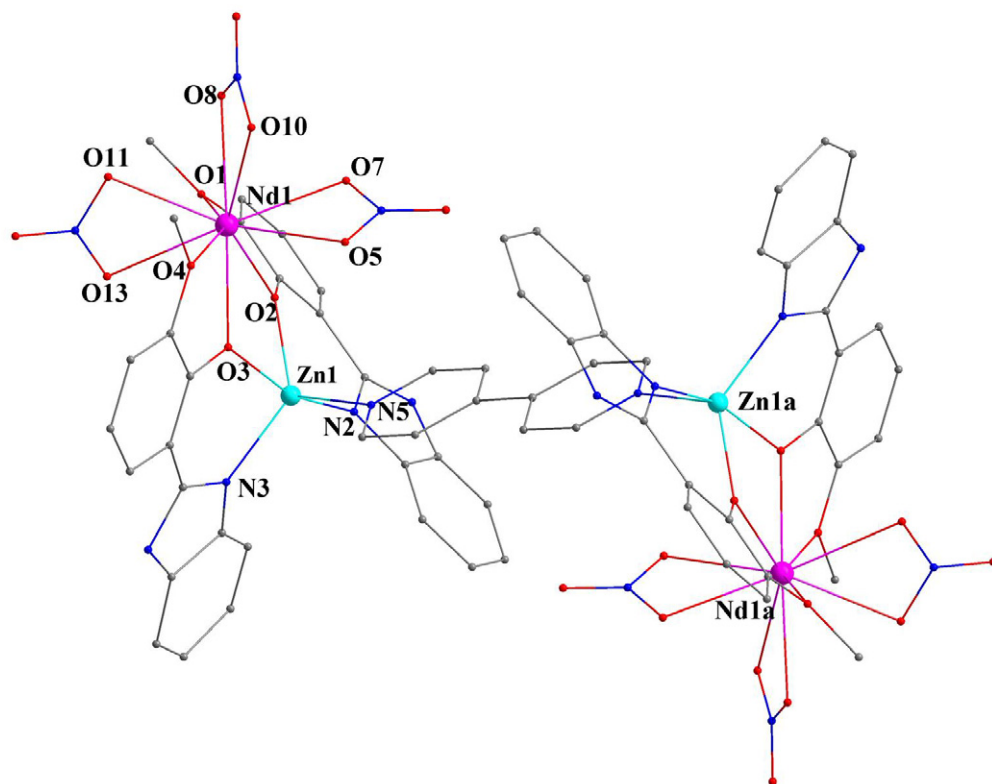


Figure 2

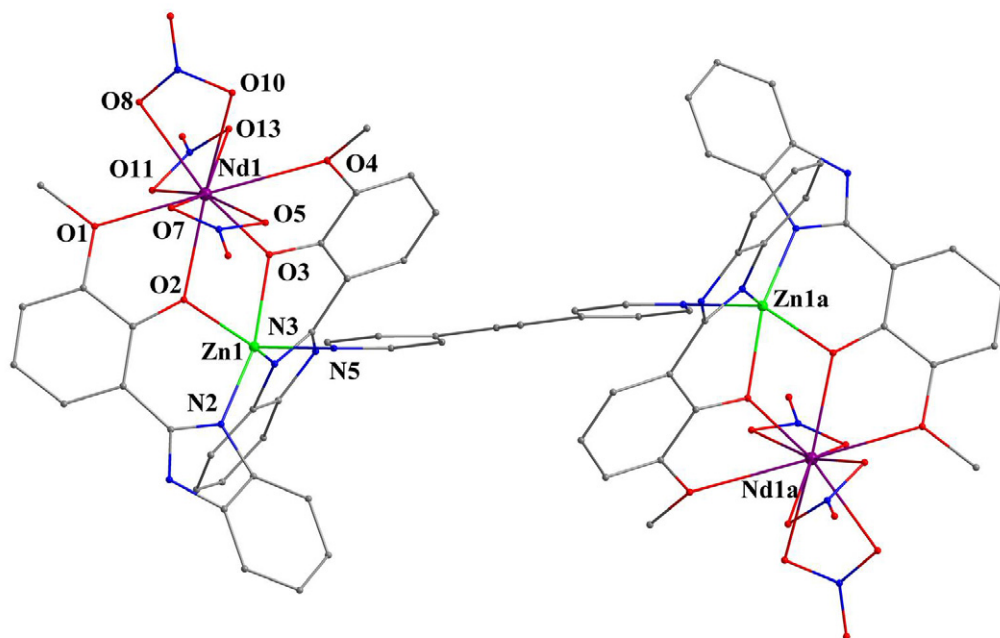


Figure 3

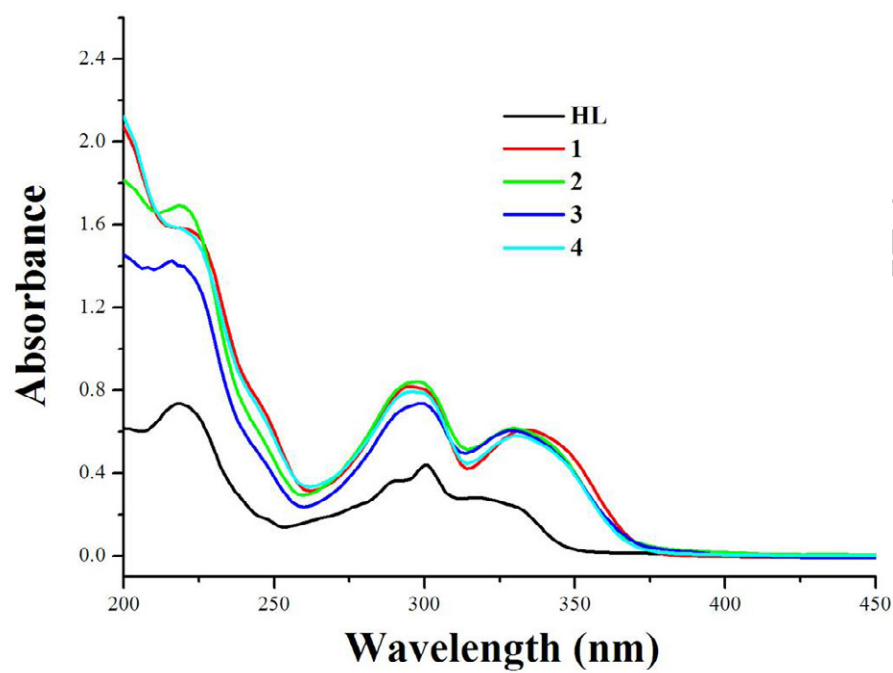


Figure 4

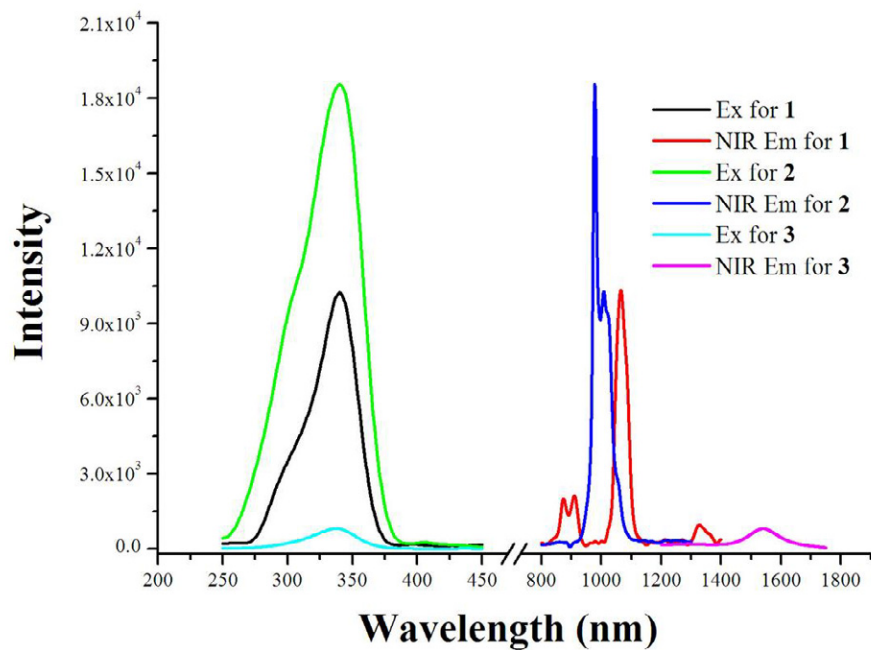


Figure 5

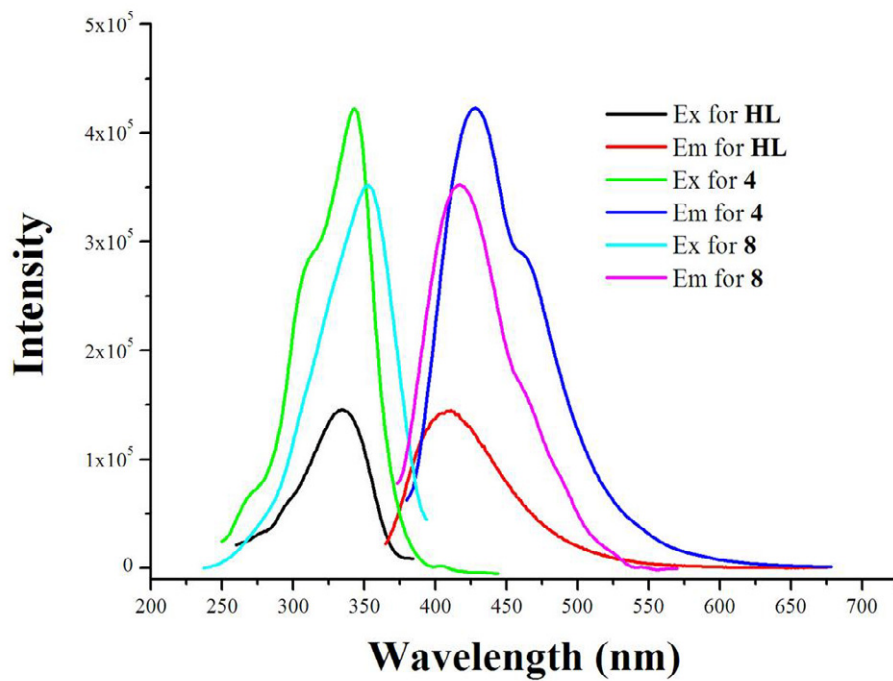


Figure 6

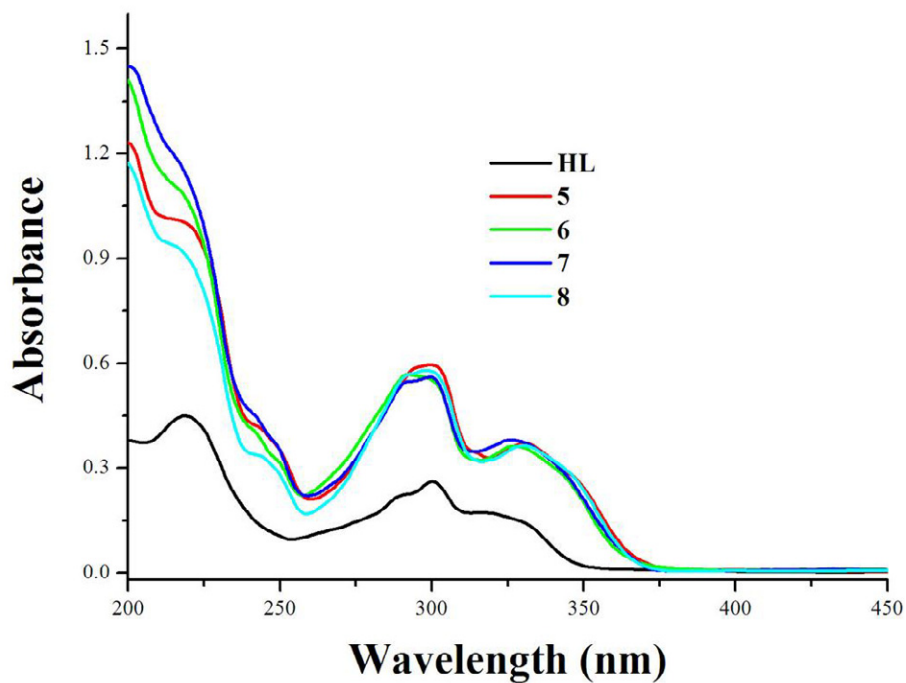
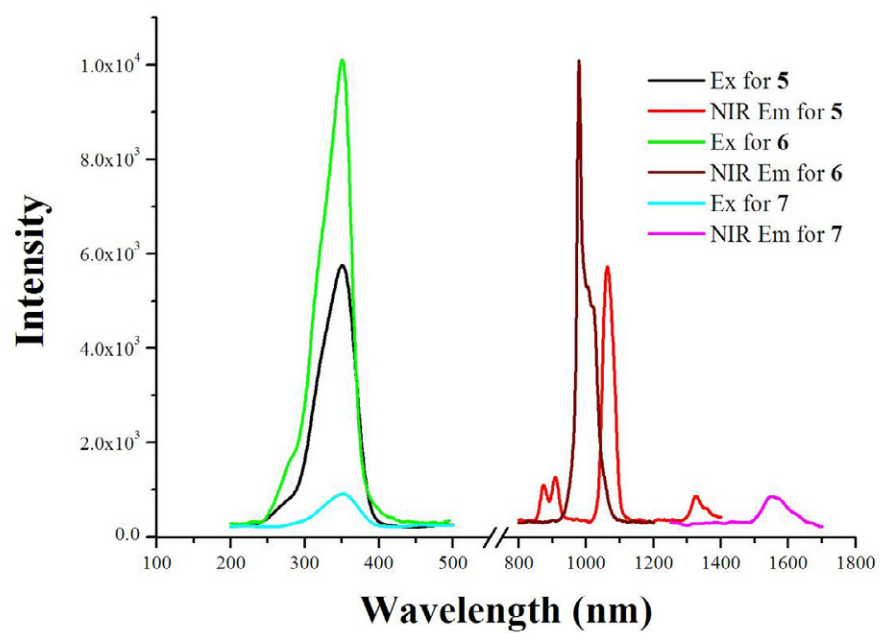


Figure 7



**Research Highlights**

- $Zn_2Ln_2$ -arrayed complexes from the benzimidazole-based ligand and two rigid 4,4'-bipyridine ligands with different spacers
- Effect of different spacers of bpy and bpe on the molecular conjugation in sensitization of NIR luminescence

ACCEPTED MANUSCRIPT

**Near-infrared (NIR) luminescent hetero-tetranuclear  $Zn_2Ln_2$  ( $Ln = Nd, Yb$  or  $Er$ ) complexes self-assembled from the benzimidazole-based HL and two rigid 4,4'-bipyridine ligands with different spacers**

Zhao Zhang, Weixu Feng, Peiyang Su, Han Liu, Yao Zhang, Zheng Wang, Tiezheng Miao, Xingqiang Lü, Daidi Fan, Wai-Kwok Wong, Richard A. Jones

Through the self-assembly of the benzimidazole-based ligand **HL** (**HL** = 2-(1H-benzo[d]imidazol-2-yl)-6-methoxyphenol) with  $Zn(OAc)_2 \cdot 2H_2O$ ,  $Ln(NO_3)_3 \cdot 6H_2O$  ( $Ln = Nd, Yb, Er$  or  $Gd$ ) and 4,4'-bipyridine ligand with different spacers (bpy, 4,4'-bipyridine or bpe, *trans*-bis(4-pyridyl)ethylene), two series of  $Zn_2Ln_2$ -arrayed complexes  $[Zn_2Ln_2(L)_4(bpy)(NO_3)_6]$  ( $Ln = Nd, \mathbf{1}; Yb, \mathbf{2}; Er, \mathbf{3}$  or  $Gd, \mathbf{4}$ ) and  $[Zn_2Ln_2(L)_4(bpe)(NO_3)_6]$  ( $Ln = Nd, \mathbf{5}; Yb, \mathbf{6}; Er, \mathbf{7}$  or  $Gd, \mathbf{8}$ ) were obtained, respectively. The result of their photophysical properties shows that the characteristic near-infrared (NIR) luminescence of  $Nd^{3+}$ ,  $Yb^{3+}$  or  $Er^{3+}$  ion has been sensitized from the excited state (both  $^1LC$  and  $^3LC$ ) of the mixed **HL** and bipyridyl ligands in both complexes **1-3** and **5-7**. Moreover, the change from bpy to bpe bridging for the fine-tuning of whole molecular conjugations, attributing to the different crossings of the two benzimidazole-based **L** ligands, has the important influence on their NIR luminescent properties.

**Near-infrared (NIR) luminescent hetero-tetranuclear  $Zn_2Ln_2$  ( $Ln = Nd, Yb$  or  $Er$ ) complexes self-assembled from the benzimidazole-based HL and two rigid 4,4'-bipyridine ligands with different spacers**

Zhao Zhang, Weixu Feng, Peiyang Su, Han Liu, Yao Zhang, Tiezheng Miao,

Xingqiang Lü, Daidi Fan, Wai-Kwok Wong, Richard A. Jones

